

# DFT on Rhodamine B Doped BIS Thiourea Cadmium Chloride (BTCC) Crystals for Nonlinear Optical Applications - A New Approach

M. Kalaiselvan<sup>1</sup>, P. Kumaresan<sup>2</sup>

<sup>1,2</sup> P.G & Research Department of Physics, Thiru.A.Govindasamy Government Arts College, Tindivanam - 604 307, Tamil Nadu, India.

**Abstract:** The stability of Bis Thiourea Cadmium Chloride (BTCC) single crystal was improved by doping Rhodamine B. The stability and charge delocalization of the molecule were also studied by natural bond orbital (NBO) analysis. The HOMO-LUMO energies describe the charge transfer takes place within the molecule. Molecular electrostatic potential has been analyzed. The developments try in extensive scale with this enhanced pH qualities is required to yield mass crystal appropriate for laser combination tests and SHG device applications. The optical, DFT studies and non-linear optical properties of the dye doped crystals were analyzed.

**Keywords:** Solution Growth, BTCC crystals, DFT, Homo- Lumo Studies, SHG measurements

## 1. Introduction

A nonlinear optical material has many applications like image application using photorefractive crystals, frequency multipliers and mixers, fiber optics, parameter oscillators, optical switches, etc., laser in a modern wonder, whether it is in the field of information transformation or in the field of medicine [1-5]. The interaction of laser with matter has advanced capabilities in optical spectroscopy. The discovery of laser itself is a result of crystal growth.

In recent years more emphasis is given to semiorganic materials due to their much matured NLO applications than organic materials and owing to their good transparency, chemical stability, and mechanical properties [6]. The large nonlinearity arises from the strong charge transfer and high polarisability. To enable a material to be potentially useful for NLO applications the material should be available in bulk single crystal form. Also research into the growth of large single crystals from aqueous solution is currently serving as the important avenue to general progress in understanding many fundamental concepts of crystallization [7]. Compared with inorganic NLO materials, organic materials may fulfill many of these requirements, but there are also some drawbacks with organic NLO materials such as environmental stability, poor chemical and mechanical stability, red-shift of the cut-off wavelength, low laser damage thresholds and poor phase matching properties. In order to overcome these drawbacks and improve the properties, the growth of semi-organic crystals has nowadays come into prominence [8-11].

The semi organic crystals have some advantages such as higher second order optical non-linearities, short transparency cut-off wavelength and stable physio-chemical performance over the traditional inorganic and organic crystals. Considering all the above mentioned facts, BTCC Crystals have been synthesized and grown moderately at low cost [12].

## 2. Density Functional Theory Studies on Rhodamine-B Doped BTCC Crystals

### 2.1 HOMO-LUMO energy gap and their molecular properties

Highest occupied molecular orbital (HOMO) and lowest unoccupied molecular orbital (LUMO) are very important parameters for quantum chemistry. The HOMO is the orbital that primarily acts as an electron donor and the LUMO is the orbital that largely acts as the electron acceptor [13]. The MOs are defined as eigen functions of the Fock operator, which exhibits the full symmetry of the nuclear point group, they necessarily form a basis for irreducible representations of full point-group symmetry [14]. The energies of HOMO, LUMO and their orbital energy gaps are calculated using B3LYP/6-311++G(d,p) method and the pictorial illustration of the frontier molecular orbitals and their respective positive and negative regions are shown in Figure 1 for thiourea doped with Rhodamine B, respectively. Molecular orbitals, when viewed in a qualitative graphical representation, can provide insight into the nature of reactivity, and some of the structural and physical properties of molecules. Well known concepts such as conjugation, aromaticity and lone pairs are well illustrated by molecular orbitals. The positive and negative phase is represented in red and green colour, respectively. From the plots we can see that the region of HOMO and LUMO [Fig.1] levels spread over the entire molecule and the calculated energy gap of HOMO-LUMO's explains the ultimate charge transfer interface within the molecule [15].

The frontier orbital energy gaps (EHOMO – ELUMO) in case of thiourea doped with Rhodamine B is found to be 0.01709 eV, respectively. GaussView 5.0.8 visualisation program has been utilized to construct the MESP surface, the shape of highest occupied molecular orbital (HOMO) and lowest unoccupied molecular orbital (LUMO) orbitals [16]. The electrophilicity index, which measures the stabilization in energy when the system acquires an additional electronic charge,  $\Delta N$  from the environment and is presented in terms

of the electronic chemical potential,  $\mu$  (the negative of electronegativity,  $\chi$ ) and the chemical hardness,  $\eta$  [2].

For more investigation some thermo dynamical parameters have been studied for this structure. Electrophilicity, chemical hardness, chemical potential, density of spectrum (Dos) (Fig. 2). The ionization potential is calculated as the energy difference between the energy of the molecule derived from electron-transfer (radical cation) and the respective neutral molecule;  $IP = E_{cation} - E_n$ . The EA was computed as the energy difference between the neutral molecule and the anion molecule:  $EA = E_n - E_{anion}$ . The HOMO and LUMO energy was also used to estimate the IP and EA in the framework of Koopmans' theorem [17-18]:

$$IP = -\epsilon_{HOMO} \text{ and } EA = -\epsilon_{LUMO}$$

Within the framework of the density functional theory (DFT), one of the global quantities is chemical potential ( $\mu$ ), which is measures the escaping tendency of an electronic cloud, and equals the slope of the Energy versus  $N$  (number of electrons) curve at external potential  $v(r)$ :

$$\mu = (\partial E / \partial N)_{v(r)}$$

Finite difference approximation to Chemical Potential gives,

$$\chi = -\mu = -(\partial E / \partial N)_{v(r)}$$

The theoretical definition of chemical hardness has been provided by the density functional theory as the second derivative of electronic energy with respect to the number of electrons  $N$ , for a constant external potential  $v(r)$ :

$$\eta = \frac{1}{2} (\partial^2 E / \partial N^2)_{v(r)} = \frac{1}{2} (\partial \mu / \partial N)_{v(r)}$$

Finite difference approximation to Chemical hardness gives,

$$\eta = (I - A) / 2$$

For Insulator and semiconductor, hardness is half of the energy gap ( $\epsilon_{HOMO} - \epsilon_{LUMO}$ ), and the softness is given as:

$$S = 1/2 \eta = (\partial^2 E / \partial N^2)_{v(r)} = (\partial E / \partial N)_{v(r)}$$

Electrophilicity index is a measure of energy lowering due to maximal electron flow between donor and acceptor. Electrophilicity index ( $\omega$ ) is defined as,

$$\omega = \mu^2 / 2 \eta$$

B3LYP functional used in this study has a high efficient to calculate the electronic properties for the organic studied molecule.

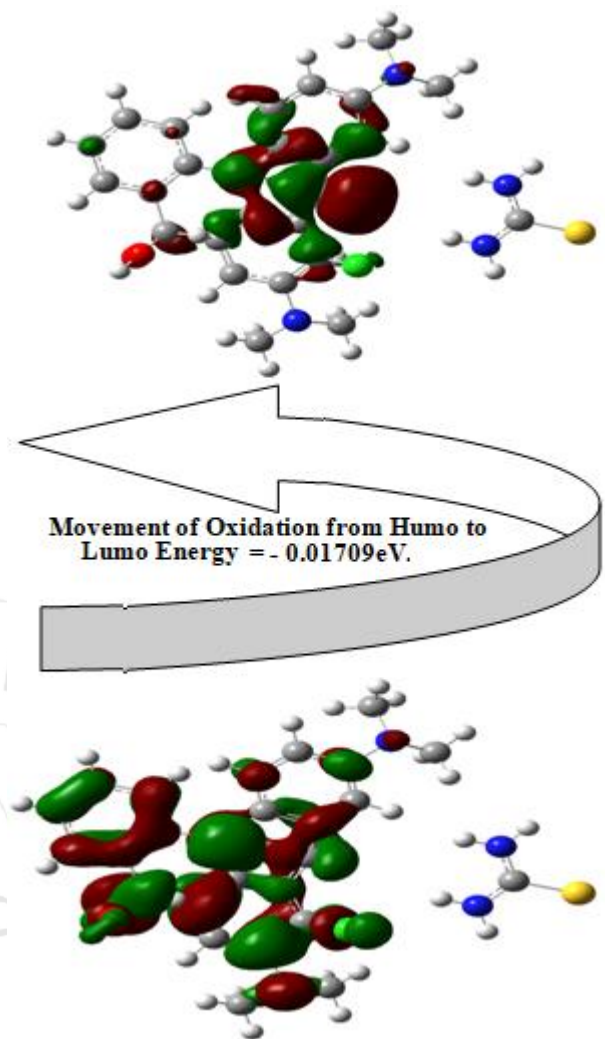


**Figure 1:** HOMO- LUMO energy gap and related molecular properties of BTCC doped with Rhodamine B.

All the calculated values of hardness, potential, softness and electrophilicity index are shown in Table 1.

**Table 1:** HOMO-LUMO energy gap and related molecular properties of thiourea doped with Rhodamine B

| Parameters                                | eV        |
|---|-----------|
| HOMO(a.u)                                 | -0.206717 |
| LUMO( a.u)                                | -0.189684 |
| Energy Gap (Eg) (a.u)                     | 0.01709   |
| Chemical Hardness( $\eta$ ) (a.u)         | 0.066853  |
| Chemical Potential ( $\mu$ ) (a.u)        | -0.223291 |
| Electronegativity ( $\chi$ ) (a.u)        | +0.223291 |
| Softness(S) (a.u)                         | 14.958192 |
| Electrophilicity Index ( $\omega$ ) (a.u) | 0.372898  |

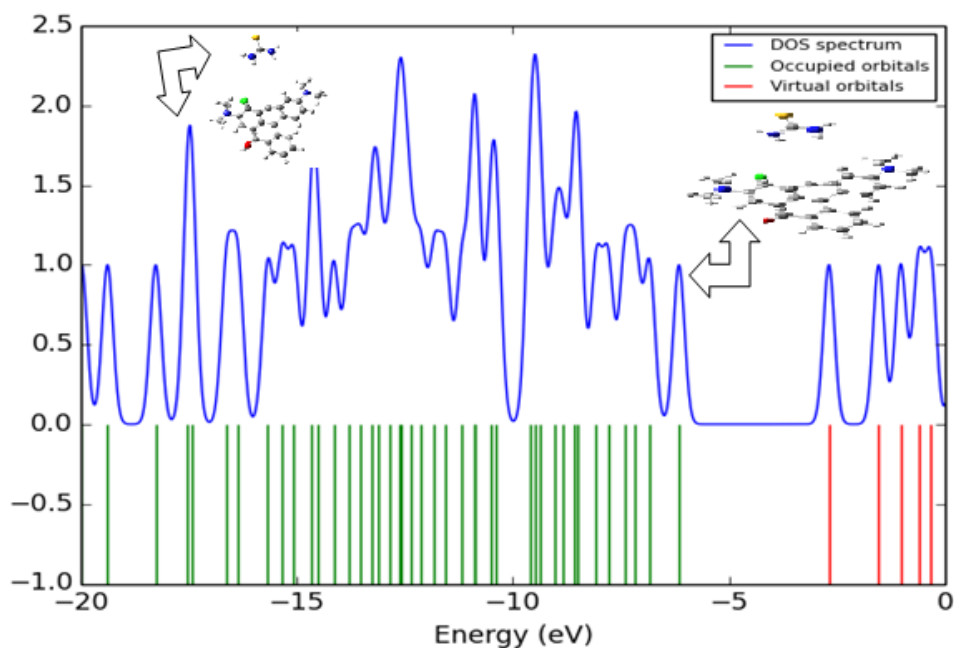


**Figure 2:** Dos spectrum of BTCC doped with Rhodamine B

## 2.2 Molecular Electrostatic Potential

The colour scheme of MESP is the negative electrostatic potentials are shown in red, the intensity of which is proportional to the absolute value of the potential energy, and positive electrostatic potentials are shown in blue while Green indicates surface areas where the potentials are close to zero [19]. The colour-coded values are then projected on to the 0.002 a.u. isodensity surface to produce a three-dimensional electrostatic potential model. Local negative electrostatic potentials (red) signal oxygen atoms with lone pairs whereas local positive electrostatic potentials (blue) signal polar hydrogens in O–H bonds. Green areas cover parts of the molecule where electrostatic potentials are close to zero (C–C and C–H bonds) [Figs(3),(4)&(5)]. Total electrostatic potential as well as mapping of different orientation for thiourea doped with Rhodamine B and the contour mapping for different degrees (15°, 30°, 45°, 60°).

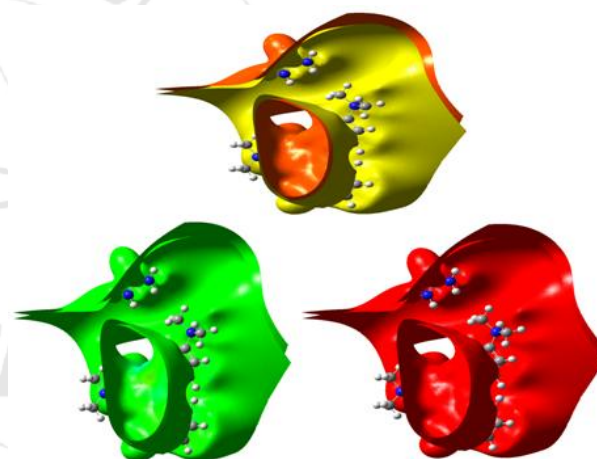


**Figure 4:** The molecular electrostatic potential surface of different orientation for BTCC doped with Rhodamine B.

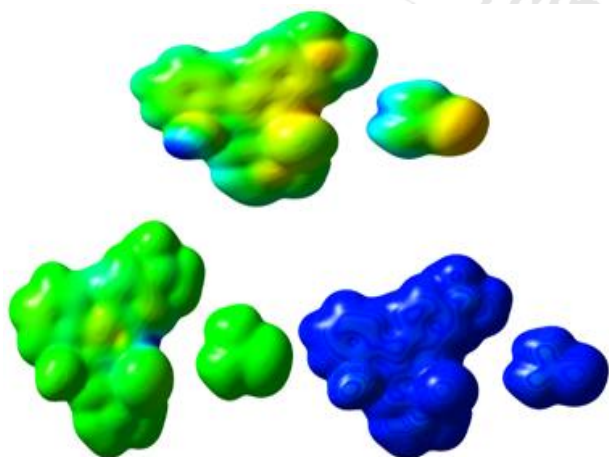


**Figure 3:** The total electron density surface of different orientation for BTCC doped with Rhodamine B.



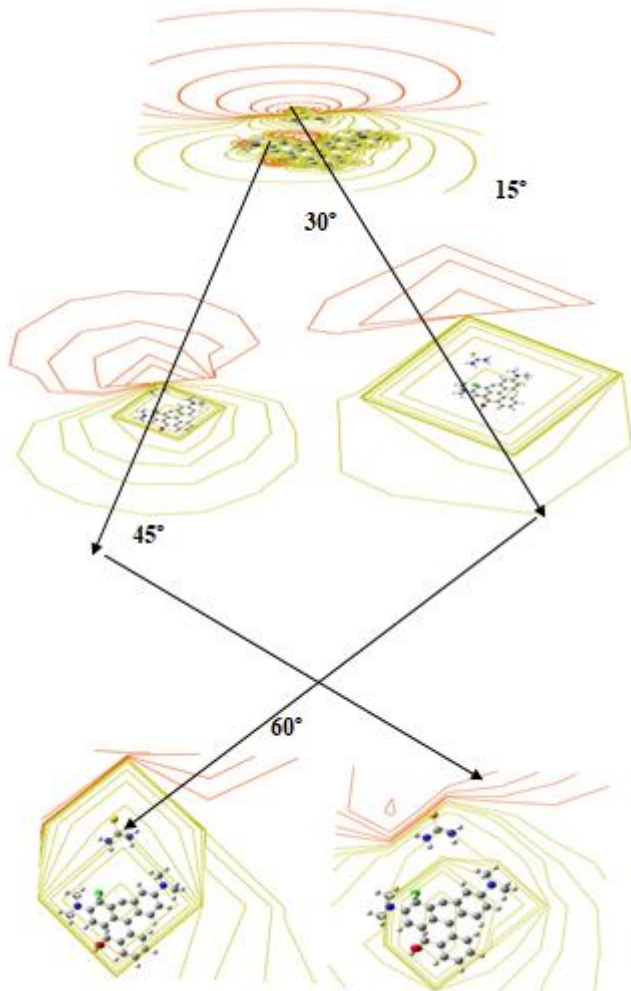


**Figure 5:** The contour map of electrostatic potential surface of different orientation for thiourea doped with Rhodamine B.

**Table 2:** Thermodynamic properties of thiourea doped with Rhodamine B determined at different temperatures with B3LYP/6-311++G(d,p) level.

| T (K)   | S (J/mol.K) | C <sub>p</sub> (J/mol.K) | ΔH <sub>0→T</sub> (kJ/mol) |
|---------|-------------|--------------------------|----------------------------|
| 100.00  | 275.97      | 58.87                    | 4.19                       |
| 200.00  | 330.74      | 107.40                   | 12.37                      |
| 298.15  | 384.56      | 167.23                   | 25.79                      |
| 300.00  | 385.60      | 168.40                   | 26.11                      |
| 400.00  | 442.49      | 228.95                   | 46.02                      |
| 500.00  | 499.33      | 280.77                   | 71.60                      |
| 600.00  | 499.33      | 280.77                   | 71.60                      |
| 700.00  | 554.37      | 322.69                   | 101.85                     |
| 800.00  | 656.17      | 383.77                   | 172.91                     |
| 900.00  | 702.72      | 406.41                   | 212.45                     |
| 1000.00 | 746.55      | 425.35                   | 254.07                     |

### 2.3 Temperature dependence of Thermodynamic properties

The temperature dependence of the thermodynamic properties heat capacity at constant pressure (C<sub>p</sub>), entropy (S) and enthalpy change (ΔH<sub>0→T</sub>) for DPK were also determined by B3LYP/6-311++G(d,p) method and listed in Table 2. The Figures 6-8 depicts the correlation of entropy (S), heat capacity at constant pressure (C<sub>p</sub>) and enthalpy change (ΔH<sub>0→T</sub>) with temperature along with the correlation equations[21-24]. From Table 2, one can find that

the entropies, heat capacities, and enthalpy changes are increasing with temperature ranging from 100 to 1000 K due to the fact that the molecular vibrational intensities increase with temperature [Figs.(6),(7) & (8)]. These observed relations of the thermodynamic functions vs. temperatures were fitted by quadratic formulas, and the corresponding fitting regression factors (R<sup>2</sup>) are all not less than 0.9995. The corresponding fitting equations for thiourea doped with Rhodamine B are

$$S = 257.977 + 0.5 T - 1.408 \times 10^{-4} T^2$$

$$C_p = 79.816 + 0.333 T - 2.478 \times 10^{-4} T^2$$

$$\Delta H = -46.658 + 0.274 T + 1.293 \times 10^{-4} T^2$$

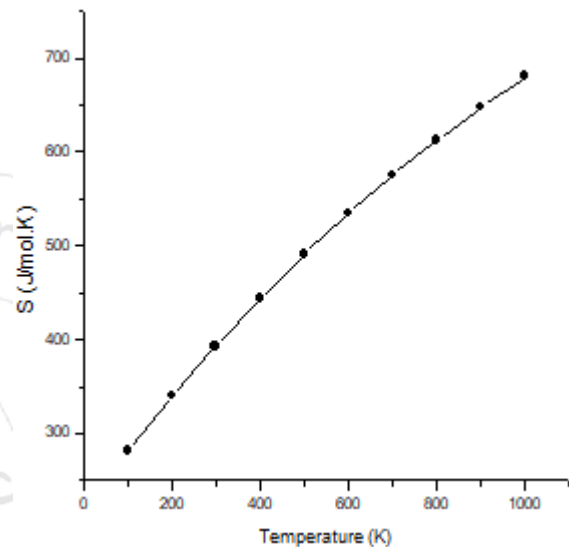


**Figure 6:** Entropy(S) of Rhodamine B doped BTCC

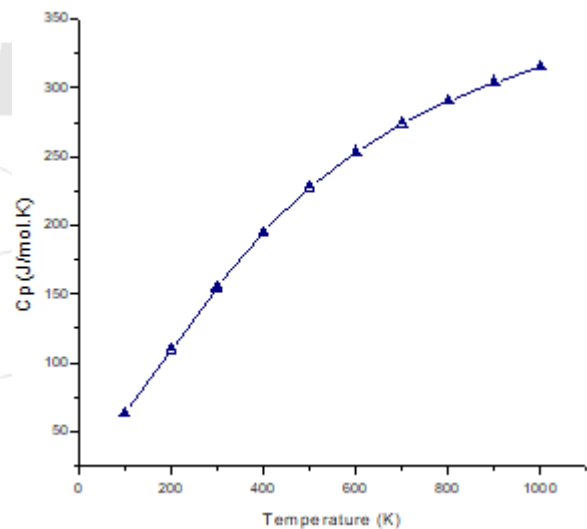


**Figure 7:** Constant Pressure (C<sub>p</sub>) of Rhodamine B doped BTCC

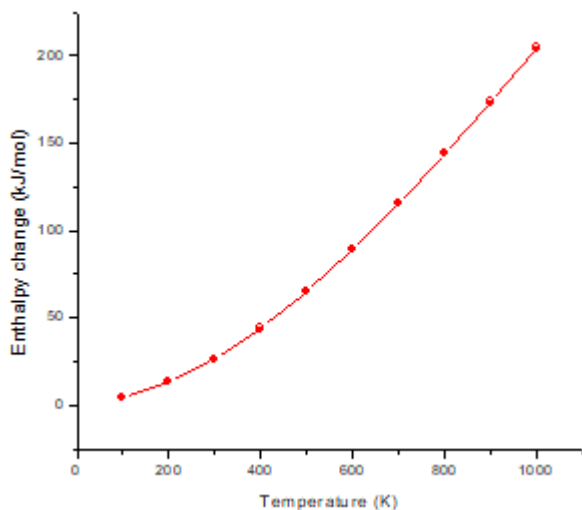


**Figure 8:** Enthalpy change of Rhodamine B doped BTCC

### Nonlinear Optical Studies

The dye doped BTCC crystals are used for the generation of second harmonics of Nd-based near-infrared solid-state lasers. Measurements were made using the Kurtz and Perry powder method[25]. The fundamental of an Nd : YAG laser (1064 nm) can be converted to 532 nm of second harmonic or its 355 nm of third harmonic or its 266 nm of fourth harmonic by using BTCC crystals. The performance of these frequency conversion devices can be seriously degraded if there are defect-associated absorption bands in the crystal which overlap the fundamental pump wavelength or one of the output wave lengths [26]. Thus, it is important to identify and characterize all potentially harmful absorption bands in non-linear optical crystals [27]. In order to confirm the suitability of the doped BTCC crystal, the non-linear applications, harmonic generation was tested using the Nd-YAG laser. A small crystal was placed on the sample holder and the YAG laser beam was made to pass through the crystal and the output conversion of input as green light SHG was analyzed.

### 3. Conclusion

The dye doped BTCC crystals are used for the generation of second harmonics of Nd-based near-infrared solid-state lasers. The fundamental of an Nd:YAG laser (1064 nm) can be converted to 532 nm of second harmonic or its 355 nm of third harmonic or its 266 nm of fourth harmonic by using BTCC crystals. The performance of these frequency conversion devices can be seriously degraded if there are defect-associated absorption bands in the crystal which overlap the fundamental pump wavelength or one of the output wave lengths. Thus, it is important to identify and characterize all potentially harmful absorption bands in non-linear optical crystals.

In order to confirm the suitability of the doped BTCC crystal, the non-linear application, harmonic generation was tested using the Nd-YAG laser. The HOMO– LUMO energy gap calculated at the B3LYP/6-311++G(d,p) level reveals the chemical activity and kinetic stability of the molecule. The large negative ESP is observed at oxygen atom in the compounds and this starts to spread near hydrogen atom under the increase of field. The NBO analysis indicates the

intramolecular charge transfer between the bonding and antibonding orbitals. The NBO analysis indicates the intramolecular charge transfer between the bonding and antibonding orbitals. This implies that the electrophilic attack is also taking place at hydrogen atom as field increases. The corresponding maps from the theoretical analysis explain similar features. Single crystals grown by the various methods need to be characterized to assess the suitability of the crystal for various applications including NLO applications. A sample of BTCC, also powdered was used for the same experiment as a reference material in the SHG measurement. It was found that the frequency doubling efficiency of the doped BTCC was better than KDP.

### References

- [1] B. Latha , P. Kumaresan, S. Nithiyantham , K. Sambathkumar, Journal of Molecular Structure 1142 (2017) 255.
- [2] P.M. Ushasree and R. Jayavel, Optical Materials, 21(2002) 599.
- [3] J. Pricilla Jeyakumari, J. Ramajothi and S. Dhanuskodi, J. Cryst. Growth, 269( 2004) 558.
- [4] S. Selvakumar, J. Packiam Julius, S.A. Rajasekharan A. Ramanand and P. Sagayaraj, Mater. Chem. Phys. 89(2005) 244.
- [5] S. Aripnammal, R. Selva Vennila, S. Radhika and S. Arumugam, Cryst. Res. Technol., 40(2005) 896.
- [6] S. Ravi and P. Subramanian, Solid State Sciences, 9 (2007) 961.
- [7] R. Uthrakumar, C. Vesta, C. Jusin Raj, S. Dinakaran, Rani Christu Dhas and S. Jerome Das, Crys. Res. Technol., 43(2008) 428.
- [8] N.R. Dhumane, S.S. Hussaini, V.G. Dongre, P.P. Karmuse and M.D. Shirsat, Crys. Res. Technol., 44(2008) 269.
- [9] J.J. Jang, S.J. Luo, L. Yi and A. Laref, Physica B. Condensed Matter., 408(2013) 175.
- [10] M. Senthilkumar and C. Ramachandraraja, Optik-International Journal for Light and Electron Optics. 124(2013) 1269.
- [11] P.M. Ushasree, R. Jayavel and P. Ramaswamy, Mater. Sci. Eng., B65(1999) 153.
- [12] H. Lipson and H. Steeple, Interpretation of X-ray Powder Diffraction Patterns, Mac Millian, New York, 1970.
- [13] S.K. Kurtz and T.T. Perry, J. Appl. Phys., 39(1968) 3798.
- [14] A. Anne Assencia and C. Mahadevan, Bull. Mater. Sci., 28, (2005)415.
- [15] S. Goma, C.M. Padma and C.K. Mahadevan, Mater. Lett., 60, (2006) 3701.
- [16] M. Priya and C.K. Mahadevan, Physica B 403(2008) 67.
- [17] S. Selvakumar, S.A. Rajasekar, K. Thamizharasan, S. Srivanesan, A. Ramanand and P. Sagayaraj, Mater. Chem. Phys., 93(2005) 356.
- [18] Y.L. Fur, R. Masse, M.Z. Cherkaoui and J.K. Nicoud, Z. Kristallogr, 210(1975) 856.
- [19] V. Venkataramanan, C.K. Subramanian and H.L. Bhat, J. Appl. Phys., 11(1995) 6049.
- [20] V. Venkataramanan, H.L. Bhat, M.R. Srinivasan, P. Ayyub and M.S. Multani, J. Raman Spectrosc., 28(1997) 779.

- [21] J. Bunget and M. Popeseu, *Physics of Solid Dielectrics* (Elsevier, New York, 1984)
- [22] C. Kittel, *Introduction to Solid State Physics* (7th edn) John Wiley and Sons, Singapore, 2005.
- [23] L.B. Harris and G.J. Vella, *J. Chem. Phys.*, 58, 1973, 4550.
- [24] P. Varotsos, *J. Phys. Lett.* 39(1978)79.
- [25] L.B. Harris and G.J. Vella, *J. Chem. Phys.*, 58(1973) 4550.
- [26] V. Venkataramanan, S. Maheswaran, J.N. Sherwood and H.L. Bhat, *J. Cryst. Growth*, 179(1997) 605.
- [27] D. Cecily Mary Glory, K. Sambathkumar, R. Madivanane, G. Velmurugan, R. Gayathri, S. Nithiyantham, M. Venkatachalapathy, N. Rajkamal, *J of Molecular Structure* 1163 (2018) 480.

